

Slow light propagation via saturable absorption of acetylene in hollow-core photonic crystal fiber

Petr Agruzov · Alexander Shamray ·
Manuel Ocegueda Miramontes · Eliseo Hernández Hernández ·
Serguei Stepanov

Received: 28 January 2012/Revised: 11 May 2012/Published online: 18 September 2012
© Springer-Verlag 2012

Abstract We report experimental results on saturable absorption of acetylene (C_2H_2) confined to a hollow-core photonic crystal fiber (PCF). In our experiments, we utilized a 3-m long PCF with a 10- μ m hollow core coupled to SMF-28 pigtailed at both ends. The 30–70-ns laser pulses of the Watt scale peak power at the wavelength $\lambda = 1528.015$ nm of the P5 line of $\nu_1 + \nu_3$ combinational band of acetylene were used. The saturation power at the center of the Doppler broadened (≈ 520 MHz) absorption line was observed to grow in the range 0.15–1.2 W in the acetylene pressure interval 0.07–0.7 mbar which was evaluated from the cell optical absorption. The slow light propagation of the 30-ns saturating laser pulses with maximal fractional delay of ≈ 0.1 was experimentally observed. Optimal input pulse power in this experiment grew with the cell optical density following growth of the saturation power.

1 Introduction

Low-pressure acetylene (C_2H_2) is known to be a source of stable and narrow absorption lines suitable for the light frequency stabilization in the 1.5 μ m wavelength region (see, e.g., [1, 2]). Recent burst of interest was caused by the reported [3–5] observation of the nonlinear resonance

interactions in the acetylene confined to hollow-core photonic crystal fibers (PCF). This new experimental configuration has enabled, in particular, reduction of the saturation cw light power to a fraction of a Watt [4, 5]. As a result, various nonlinear effects promising for practical applications, and in particular, the electromagnetically induced transparency [4, 6, 7] and the slow light propagation [4, 7] were reported in such fiber-based acetylene cells. Recently they were also utilized for mode locking [8] and wavelength stabilization [9] in erbium-doped fiber lasers.

In this paper, we report detailed data on dependence of the saturation power for acetylene in the hollow-core PCF on the gas pressure. We employ a pumped-through SMF28 fiber pigtailed PCF cell, which needs neither vacuum chambers nor bulk coupling optics. The experiments were performed with the nanosecond laser pulses with up to 10 W peak powers. This allowed us to observe the propagation of the slowed down 30-ns light pulses directly at the saturating light wavelength with the fractional delay up to ≈ 0.1 . This value is comparable with that achieved recently in the acetylene filled PCF in a more complicated configuration of electromagnetically induced transparency where two different resonance wavelengths are utilized. Note that slow/fast light propagation due to direct saturation of the optical absorption/gain was also reported recently in the bulk laser crystals [10], semiconductor waveguides [11], and in erbium-doped fibers [12].

2 Experimental setup and results

The optical part of our experimental setup is shown in Fig. 1a. As a primary source of coherent radiation, a conventional thermo-stabilized DFB laser diode with the 20 mW cw output at the wavelength centered at 1,527 nm

P. Agruzov · A. Shamray
Ioffe Physical-Technical Institute of the Russian Academy
of Sciences, Politehnicheskaja 26,
Saint Petersburg 194021, Russia

M. Ocegueda Miramontes · E. Hernández Hernández ·
S. Stepanov (✉)
CICESE, Carretera Ensenada-Tijuana 3918,
Ensenada 22860, Mexico
e-mail: steps@cicese.mx

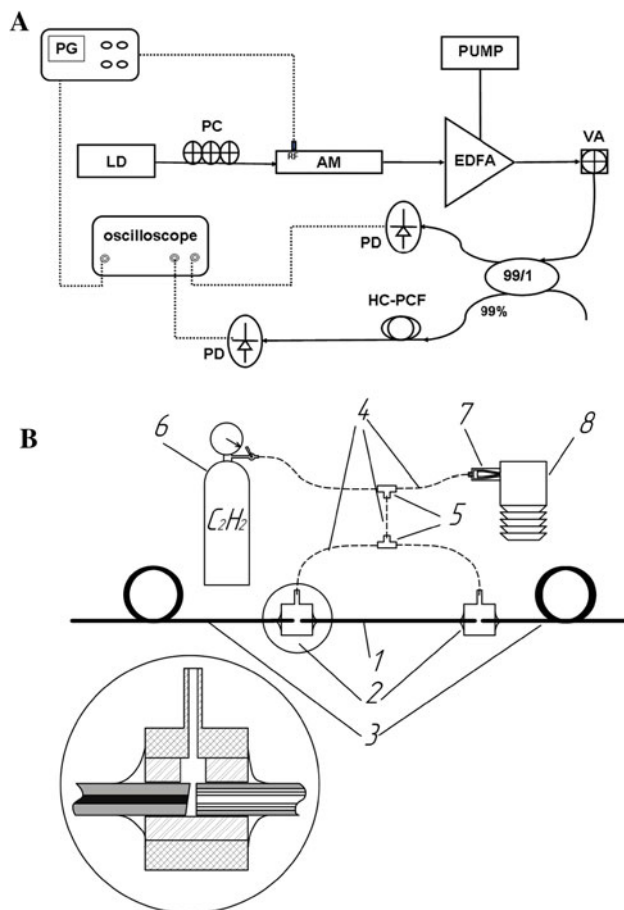


Fig. 1 **a** Schematic of the optical part of the experimental setup: *LD* temperature controlled semiconductor DFB laser tuned to 1528.015 nm, *PUMP* 980 nm semiconductor pump laser, *PG* pulse generator, *PC* polarization controller, *AM* electro-optic amplitude modulator, *EDFA* erbium-doped fiber amplifier, *VA* variable attenuator, *PD* fast photodiode, *HC-PCF* hollow-core photonic crystal fiber. **b** Schematic of the PCF acetylene cell pressure control system: 1 photonic crystal fiber, 2 gas accessible optical connectors, 3 SMF-28 single-mode fiber tails, 4 gas pipe, 5 T-shape gas connectors, 6 acetylene tank with a valve, 7 needle valve, 8 diffusion pump. *Inset* shows design of the PCF/SMF28 couplers

was utilized. Fine tuning of the generated wavelength to the wavelength 1,528.015 nm of the P5 line of $\nu_1 + \nu_3$ combinational band of acetylene was ensured via control of the laser diode temperature and pumping current. The laser spectral FWHM (full width half maximum) was evaluated to be below 5 MHz.

The linearly polarized output of the laser diode was modulated by a high-frequency electro-optic amplitude modulator with up to 33 dB contrast and the output 30–70 ns pulses with the peak power of about 6 mW were amplified by an EDF optical amplifier pumped by the 120 mW at 980 nm. This allowed us to achieve light pulses of up to 10 W peak light power at the acetylene cell input. The pulse power was controlled by a variable attenuator

and monitored via a 99/1 fiber coupler by means of a fast (15 GHz) photodiode.

The configuration of our gas filling/evacuation system and of the acetylene PCF cell is presented in Fig. 1b. The gas cell was fabricated on the basis of a commercially available HC-1550-04 hollow-core PCF (of NKT Photonics Inc.). The PCF cell was pigtailed using segments of the conventional single-mode SMF-28 fiber and terminated with FC/APC connectors. Unlike earlier reported all-fiber acetylene PCF cell [13], coupling and alignment of these two different fibers was performed inside a single ferrule (see the inset to Fig. 1b) that had a transverse notch. It was cut with a diamond saw and ensured coupling of the PCF hollow core to the gas filling/evacuation system. No anti-reflection coatings were utilized and the light transmission was 0.35 and 0.75 through the one and the other PCF-SMF connections, respectively. We attribute these light losses mainly to misalignments of the fibers' cores in the ferrules. In the presented experiments, the end of the fiber cell with the higher transmission of the PCF-SMF connection was used as the input one.

To suppress possible reflections (and unwanted Fabry-Perot effects) due to the glass-air interfaces, one end of SMF-28 fiber was cleaved at a small angle with respect to the normal. In this way, the reflection from fiber end was suppressed by approximately 10 dB down.

The procedure of the fiber cell filling with the acetylene was as follows. First, the PCF cell was evacuated using a diffusion pump to avoid possible mixing of acetylene with other contaminant gases. Then the cell was filled with acetylene by releasing the gas from the tank and letting it enter the PCF hollow core. During this process, the cell transmission spectrum was monitored to evaluate the filling of the cell with the gas in real time. This filling step was performed until the residual transmission reached the stable level that usually took about 1 h. Finally, the acetylene flow was stopped and the same vacuum system was again used to evacuate acetylene from the PCF core slowly. To control the evacuation speed and to set the desirable pressure level, a needle valve at the pump input was used. This also allowed us to prevent from any possible intrusion and outgassing in the vacuum system.

The real-time evaluation of the acetylene pressure in the PCF cell was also performed in our experiments optically, via monitoring the intensity of the gas P5 absorption line. The acetylene-associated transmission T was evaluated as a ratio between the transmitted power inside the acetylene absorption peak and that outside of it. This was done to eliminate the light losses due to non-ideal PCF-SMF fiber connections and due to possible excitation of higher PCF spatial modes. Figure 2a shows the cell optical density $OD = -\ln(T)$ profiles observed after 55, 62, and 85 min of the gas evacuation from the cell which was initially filled

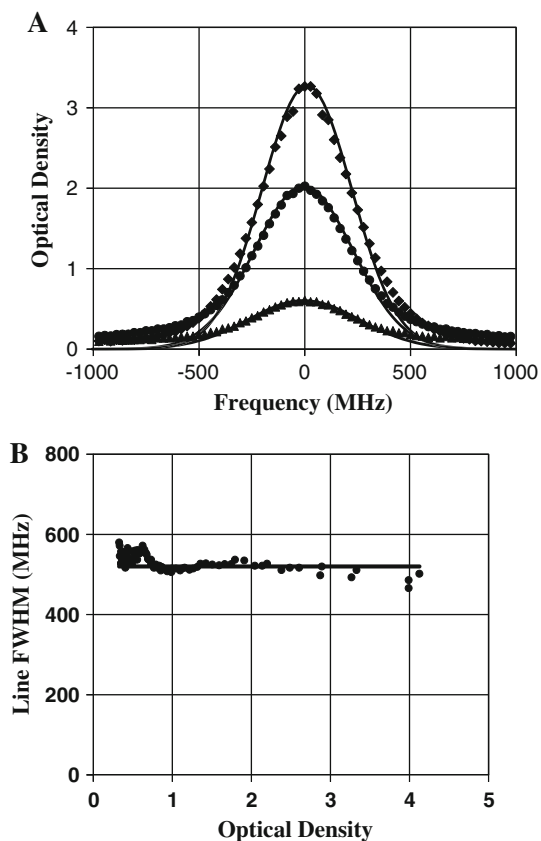


Fig. 2 **a** Typical acetylene cell optical absorption spectral profiles observed after 55, 62, and 85 min of the gas evacuation approximated by Gaussian curves with maximal optical density: *diamond* 3.3, *circle* 2.0, and *triangle* 0.6. **b** Low power (i.e. not saturated) acetylene cell optical absorption FWHM as a function of the cell optical density

with the acetylene under pressure of ≈ 2 atm. To obtain the presented curves the wavelength scan nonlinearity was corrected using the fiber loop etalon [14] with 27.8 MHz free spectral range. One can see from Fig. 2a that the optical density spectral curves can be approximated by Gaussian-like profiles beginning from the very moment when we can reliably evaluate the minimal transmission in the acetylene line (OD = 3–4). The FWHM spectral width of the profiles proved to be nearly constant and was about 520 MHz (see Fig. 2b).

To measure the cell stationary transmission as a function of the peak input light power, we used input 70-ns pulses of the trapezoidal shape with approximately flat tops (see Fig. 3). Figure 4a shows a typical dependence of the cell optical density on the peak light power for one particular gas pressure. The optical saturation of the cell absorption is clearly seen from this dependence without any special processing. Similar curves were obtained for different initial unsaturated optical densities OD (in the range of = 0.35–3.3) determined by the acetylene pressure at the moment of the measurement, see Fig. 4b.

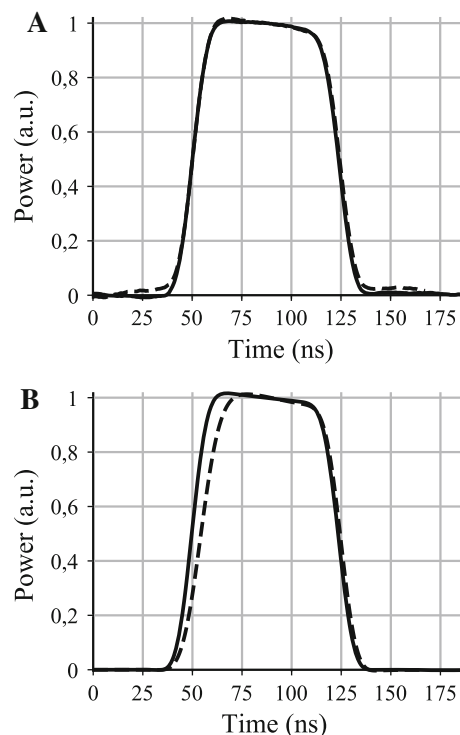


Fig. 3 Transmission of the 70 ns light pulses through the acetylene cell: **a** without saturation (at low input power), and **b** with saturation at the first pulse front. Pulse shapes (solid line input pulse, dash line output pulse) are presented in the normalized form

Distortions of the 70-ns pulses at the acetylene cell output are shown in Fig. 3b. Note that the most significant changes were observed at the fronts of the detected output profiles mainly. This indicates, in particular, that shorter pulses are required for more impressive, slow light experiments. Figure 5 illustrates propagation of the 30-ns pulses, for which the temporal pulse delay (evaluated as displacement of center of the pulse half-maximum level) is clearly observable. This figure also illustrates the output pulse distortions and time delay change with the increasing peak power of the input pulse.

3 Discussion

Let us start our discussion with the analysis of the absorption profiles. As noted above, Fig. 2a shows that the experimentally observed profiles with maximal optical densities OD = 0.35–3.3 are well approximated by Gaussian profiles with nearly constant spectral FWHM of about 520 MHz. Such absorption profiles of acetylene at room temperature are usually associated with conventional Doppler mechanism of inhomogeneous broadening [4]. The constant FWHM of the spectral profile also indicates that the pressure-induced homogeneous line broadening is

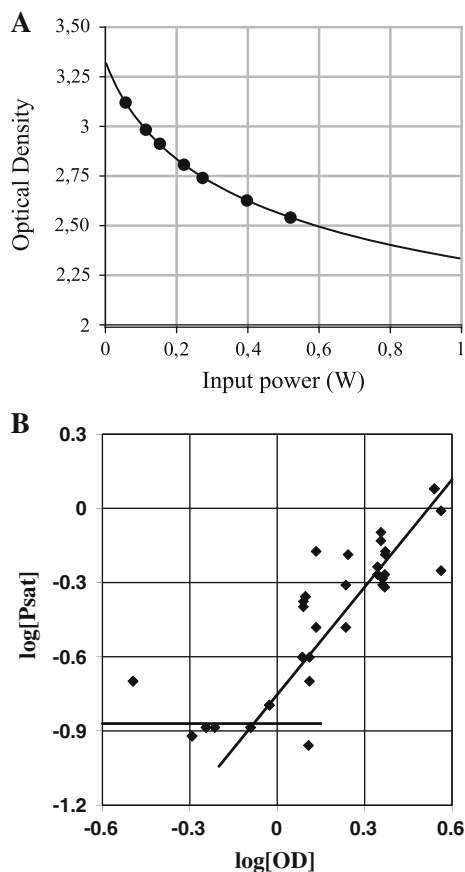


Fig. 4 **a** Optical density of the acetylene cell as a function of input pulse peak power. Fitting with Eq. (2) using corresponding initial optical density results in saturation power $P_{\text{sat}} = 0.8$ W. **b** Dependence of the evaluated saturated power (measured in Watts) versus initial optical density of the acetylene cell

appreciably smaller than the experimentally observed spectral width.

Simulation of optical transmission of the cell using the HITRAN database shows that the average acetylene pressure inside the fiber core is changing in the range 0.07–0.7 mbar for the above-mentioned optical density range. The literature data [2] show that the pressure-induced line width is described by a linear dependence with the rate coefficient about 13.0 MHz/Torr, or 9.9 MHz/mbar for the P5 acetylene line. Using these data, the pressure-induced linewidth change can be estimated to be in 0.69–6.9 MHz range only.

It is also well known (see e.g. [1]) that there is another mechanism of the homogeneous broadening of the acetylene lines in the PCF cell, namely, collisions of the gas molecules with the internal walls of the fiber hollow core. The corresponding linewidth can be approximately evaluated as an inverse average time of flight of the molecules between the capillary walls. For the fiber core diameter 10 μm and the average thermal velocity of the acetylene

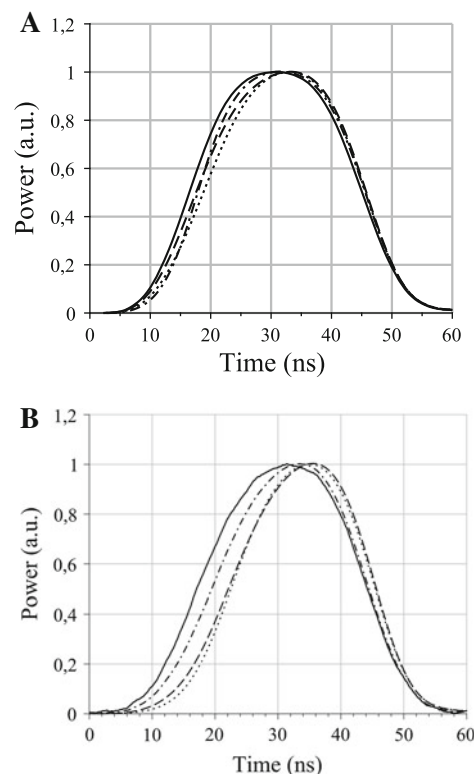


Fig. 5 The 30 ns pulse shapes observed at the acetylene cell output at different input pulse peak powers (all pulses are presented in the normalized form). Acetylene pressure: **a** 0.3 mbar (input power, W: dashed line 0.14, dot line 0.4, dash-dot line 3.5), and **b** 1 mbar, (input power, W: dash-dot line 0.65, dashed line 1.7, dot line 3.6). The normalized profile of the input pulse is shown by solid lines

molecules at ≈ 300 K of 494 m/s, this value can be roughly estimated as ≈ 40 MHz. Note that in the experiments on the electromagnetically induced transparency reported in [4] the FWHM of the homogeneously broadened acetylene absorption line R16 in the 12 μm capillary was estimated to be ≈ 44 MHz. The authors of [5] also reported the transit time broadening around 44 MHz for the P9 acetylene absorption line in a PCF with a hollow-core diameter of 10 μm .

To analyze the cell transmission as a function of the input power (Fig. 4a), we used the well-known equation for propagation of the saturating light power in a saturable medium:

$$\frac{dP}{dz} = -P \frac{\alpha_0}{1 + P/P_{\text{sat}}}, \quad (1)$$

where α_0 and P_{sat} are the initial (not saturated) optical absorption and the saturation power of the acetylene cell, respectively. To take into account that the input light power is distributed non-uniformly along the fiber length because of considerable light absorption in the fiber cell, we used in our fits the analytic solution (see e.g. [15]) of the above

equation that yields the following stationary value of the transmission coefficient:

$$T = \frac{P_{\text{in-line}}}{P_{\text{out-line}}} = \frac{P_{\text{sat}}}{P_{\text{in}}} W \left[\frac{P_{\text{in}}}{P_{\text{sat}}} \exp \left(-\alpha_0 L + \frac{P_{\text{in}}}{P_{\text{sat}}} \right) \right], \quad (2)$$

where the Lambert function $W(x)$ is the solution of equation $W(x) * \exp[W(x)] = x$. An example of an approximation of one set of the experimental data by this theoretical dependence is presented in Fig. 4a. The saturation power is derived from this approximation as a fitting parameter. The results of such fits for different gas pressures are summarized in Fig. 4b in the form of dependence of the evaluated saturation power on the cell initial optical density.

It is generally accepted that when the pressure-induced mechanism of the homogeneous broadening is dominant, the saturation power grows quadratically with pressure [1]. On the opposite, when the homogeneous line width is governed by collisions with the walls, the saturation power is independent of pressure. Furthermore, the high-pressure part of the experimental dependence presented in Fig. 4b can be approximated by the power dependence close to the quadratic one, while the saturation power (≈ 0.15 W) evaluated for the low-pressure part can be considered as approximately constant. The transition from these two different regimes of the pressure dependence is observed at the acetylene pressure corresponding to the cell optical density ≈ 0.7 .

Qualitatively, the experimentally observed dependence of the saturating power presented in Fig. 4b corresponds to the above-mentioned theoretical predictions. The main problem is, however, that experimentally the transition between two mentioned above characteristic regions of this dependence is observed at significantly lower acetylene optical absorption (i.e. the partial acetylene pressure) as it is expected. Indeed, the pressure-induced and the collision-induced spectral widths are to be equal at approximately ≈ 4.0 mbar, which is somewhat above the estimated acetylene pressure range used in our experiments.

We attribute this discrepancy to the acetylene collisions with the residual air molecules [16], which, as we believe, are inevitably present inside our all-fiber gas cell with several vacuum connections. Note that such collisions increase the homogeneous spectral width, but do not influence the maximal acetylene absorption, which was used above in estimate of the acetylene partial pressure. This hypothesis obviously need more detailed investigation, but our above-presented evaluations mean that all experiments which involve saturation of the acetylene at relatively high gas pressure are to be rather sensitive to the admixture of the air in the PCF acetylene cell.

As it was mentioned above, the light pulse duration of about 70 ns seems to be too large to observe an effective slow light propagation. Indeed, only a small change in the

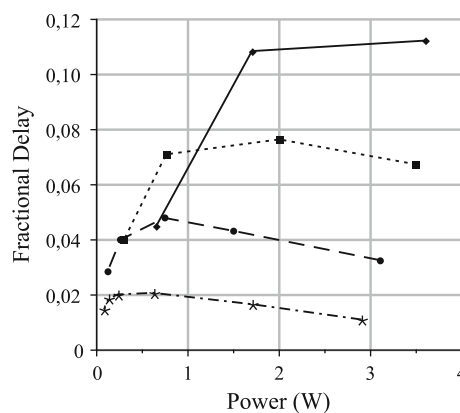


Fig. 6 Fractional pulse delay as a function of the peak incident pulse power observed for different pressures, mbar: 0.1 (asterisk), 0.3 (circle), 0.7 (square), and 1.0 (diamond)

output pulse front can be traced in Fig. 3b. The pulse duration of 30 ns comparable to the expected average time of flight between the core internal walls utilized in the below-presented experiments seems to be closer to the optimal one. In fact, experimentally we observed that, as the peak power input grows, the transmitted 30 ns light pulses are getting narrower and their maxima shift to the right, which corresponds to larger arrival times, or the pulse delay (see Fig. 5).

Figure 5 also shows that the maximum fractional pulse delay (i.e., the time delay of the middle of the pulse half-maximum level normalized to the input pulse width) is higher for large optical cell densities. At lower input pulse powers, no gas saturation occurs, and the output pulse shape does not change significantly. When the input pulse power approaches the saturation power, the time delay is maximal. If the pulse power continues to grow, the pulse delay diminishes because of the excessive saturation of the gas. Experimentally the maximum pulse delay occurs at a specific input power for each pressure. For example, at the 1 mbar pressure the longest delay takes place at 3.6 W, at 0.7 mbar the longest delay is observed at 2 W, and at 0.3 mbar—at 0.74 W—see Fig. 6. This trend, first of all, reflects the change of the saturation power with the gas pressure.

Note that earlier the slow light propagation in the acetylene PCF cells was observed only via the effect of the electromagnetically induced transparency [4, 7], when a narrow transmission peak was produced by illuminating the cell with an auxiliary laser with a shifted wavelength. In our case we used only one laser source which saturates the medium at its own wavelength. The maximal fractional delay reached in our experiments was about 0.1, which is comparable with similar results obtained in the above-mentioned experiments on electromagnetically induced transparency in acetylene PCF cells. In our experiments,

this fractional delay was observed for the initial acetylene cell optical density about 3.3 and for the incident peak 30 ns pulse power 3.6 W.

It is interesting to note that this experimentally observed value is also very close to a simple theoretical estimate $\sim \alpha_0 L / 8\pi$ (see e.g. [17]). For a typical value $\alpha_0 L = 2$, this gives us the maximum fractional delay of about 0.08. The theoretical estimate was obtained in the above-mentioned paper as a result of consideration of a sinusoidally modulated light intensity propagating through a thin optically saturable material of low initial optical density.

4 Conclusion

Summarizing, we have reported the results on saturable absorption and slow light pulse propagation in the acetylene pumped-off hollow-core PCF pigtailed cell. For the optical densities $OD < 0.7$ of the 3-m long cell (i.e. at the acetylene pressures < 0.14 mbar) the saturation power of the acetylene optical transition P5 at the wavelength 1,528.015 nm was found to be constant and approximately equal to 0.15 W. This points out that the homogeneous broadening via collisions with the hollow-core fiber walls is dominating under these experimental conditions. The maximal pulse fractional delays in the experiments of the slow light propagation of about ≈ 0.1 was observed for the 30 ns pulses of the saturating light and proved to be in a reasonable agreement with the theoretical evaluation based on saturable optical density (≈ 3.3) of the acetylene cell. This value is also comparable with the earlier reported experimental results on slow light propagation via electromagnetically induced transparency in similar acetylene PCF cells.

References

1. M. de Labachellerie, K. Nakagawa, M. Ohtsu, Ultranarrow $^{13}\text{C}_2\text{H}_2$ saturated-absorption lines at 1.5 μm . *Opt. Lett.* **19**, 840–842 (1994)
2. W.C. Swann, S.L. Gilbert, Pressure-induced shift and broadening of 1510–1540-nm acetylene wavelength calibration lines. *JOSA B* **17**, 1263–1270 (2000)
3. F. Behabid, F. Couny, J.C. Knight, T.A. Birks, P.S.J. Russell, Compact, stable and efficient all-fibre gas cells using hollow-core photonic crystal fibres. *Nature* **434**, 488–491 (2005)
4. S. Ghosh, J.E. Sharping, D.G. Ouzounov, A.L. Gaeta, Resonant optical interactions with molecules confined in photonic band-gap fibers. *Phys. Rev. Lett.* **94**, 093902 (2005)
5. J. Henningsen, J. Hald, J.C. Petersen, Saturated absorption in acetylene and hydrogen cyanide in hollow-core photonic bandgap fibers. *Opt. Express* **13**, 10475–10482 (2005)
6. F. Couny, P.S. Light, F. Benabid, P.S.J. Russell, Electromagnetically induced transparency and saturable absorption in all-fiber devices based on $^{13}\text{C}_2\text{H}_2$ -filled hollow-core photonic crystal fiber. *Opt. Commun.* **263**, 28–31 (2006)
7. N.V. Wheeler, P.S. Light, F. Couny, F. Benabid, Slow and superluminal light pulses via EIT in a 20-m acetylene-filled photonic microcell. *J. Lightwave Technol.* **28**, 870–875 (2010)
8. P.T. Marty, J. Morel, T. Feurer, Pulsed erbium fiber laser with an acetylene-filled photonic crystal fiber for saturable absorption. *Opt. Lett.* **36**, 3569–3571 (2010)
9. P.T. Marty, J. Morel, T. Feurer, All-fiber frequency-stabilized erbium doped ring laser. *Opt. Express* **18**, 26821–26827 (2010)
10. M. S. Bigelow, N. N. Lepeshkin, R.W. Boyd, Superluminal and slow light propagation in a room-temperature solid. *Science* **301**, 200–202 (2003)
11. J. Mørk, R. Kjør, M. van der Poel, K. Yvind, Slow light in a semiconductor waveguide at gigahertz frequencies. *Opt. Express* **13**, 8136–8145 (2005)
12. A. Schweinsberg, N.N. Lepeshkin, M.S. Bigelow, R.W. Boyd, S. Jarabo, Observation of superluminal and slow light propagation in erbium-doped optical fiber. *Europhys. Lett.* **73**, 218–224 (2006)
13. P.T. Marty, J. Morel, T. Feurer, All-fiber multi-purpose gas cells and their applications in spectroscopy. *J. Lightwave Technol.* **28**, 1236–1240 (2010)
14. L.F. Stokes, M. Chodorow, H.J. Shaw, All-single-mode fiber resonator. *Opt. Lett.* **7**, 288–290 (1982)
15. S. Stepanov, C. Nuñez Santiago, Intensity dependence of the transient two-wave mixing via population grating in Er-doped fiber. *Opt. Commun.* **264**, 105–115 (2006)
16. S.W. Arteaga, C.M. Bejger, J.L. Gerecke, J.L. Hardwick, Z.T. Martin, J. Mayo, E.A. McIlhattan, J.-M.F. Moreau, M.J. Pilkenton, M.J. Polston, B.T. Robertson, E.N. Wolf, Line broadening and shift coefficients of acetylene at 1550 nm. *J. Mol. Spectrosc.* **243**, 253–266 (2007)
17. S. Stepanov, E. Hernandez Hernandez, Controllable propagation of light pulses in Er-doped fibers with saturable absorption. *Opt. Lett.* **33**, 2242–2244 (2008)